



Research into the Production of Tungsten Heavy Alloys with Specific Mechanical Properties

Paweł SKOCZYLAŚ*, Zbigniew GULBINOWICZ, Olgierd GOROCH,
Katarzyna BARCZ, Mieczysław KACZOROWSKI

*Warsaw University of Technology,
Faculty of Production Engineering, Institute of Mechanics and Printing
85 Narbutta Str., 00-701 Warsaw, Poland*

**Corresponding author's e-mail address and ORCID:
pskocz@imik.wip.pw.edu.pl; <https://orcid.org/0000-0001-5295-9713>*

Received by the editorial staff on 15 August 2018

The reviewed and verified version was received on 10 December 2019

DOI 10.5604/01.3001.0013.6483

Abstract. The subject of the work discussed herein and carried out as a part of the Polish National Centre of Research and Development project titled "Development and implementation of critical technology demonstrators for the new generation of 120 mm tank artillery ammunition" are the results of a research into the influence of LPS (*Liquid Phase Sintering*) parameters and heat treatment on the mechanical properties of W91Ni6Co3 and W91Ni6Co2.25Fe0.75 alloys, designated PR200 and PR201, respectively. The alloys, as LPS-processed and heat treated, were tested on a strength testing machine to determine their tensile strength (R_m), proof stress ($R_{p0.2}$) and elongation (A_5). The analysis of the test results resulted in a proposal of manufacturing process parameters to have the alloys tested develop specified mechanical properties.

It was found the ternary alloy with chemical composition W91Ni6Co3 and designated PR200 was more promising in the feasibility of producing specified mechanical properties. The alloy, once sintered and heat treated in two stages, could facilitate production of a material with a tensile strength $R_m > 1400$ MPa, a yield strength $R_{p0.2} > 1350$ MPa, a minimum elongation of 11%, and an impact strength > 115 J/cm².

Keywords: tungsten heavy alloys, liquid phase sintering, high-strength tungsten heavy alloy, mechanical properties, kinetic energy penetrators, high-strength WHA.

1. INTRODUCTION

Tungsten heavy alloys (WHAs) are unique materials which combine a very high density with high strength, high plasticity (flow) and high impact strength. Given their very high melting point, WHAs are usually formed by application of powder metallurgy processes, including die pressing and sintering, where the method of choice for the latter is LPS (*Liquid Phase Sintering*). The microstructure of a WHA which has been sintered features hard tungsten grains with a near-spheroidal geometry and a size between 20 and 60 μm ; the tungsten grains are embedded in a plastic matrix, or the binder phase. The WHA matrix is usually a solid solution with the major component being nickel and a complement of dissolved additives, which include Fe, Co, Cu, Re, Ta, Mo, and W.

WHAs have found many applications in multiple industries: as balancing weights for aircraft or gyroscope components. WHAs are used for pressing dies, parts of casting moulds, vibration dampers, and vibrating components for mobile phone sound indicators. The many applications of WHAs cannot be mentioned without radiation shielding, collimator units, shielding of syringes for administration of isotope materials, spark machining electrodes, or high current contacts. WHAs have seen applications in the production of athletic and sports equipment, like golf club tips, parts of shuttlecocks and tennis rackets, and — due to their good corrosion resistance — angling weights [27-33].

A special application area of WHAs is the defence industry, where the alloys see use in the production of armour-piercing discarding sabots (APDS). where they replace DU (*Depleted Uranium*). Over the last 20 years, the research into WHAs applied in APDS sub-projectiles was focused on improving the armour-penetrating capability, the measure of which is the thickness of penetrated armour plating. The efforts at this improvement were to increase the strength of the sub-projectile material while maintaining its maximum possible density. The criterion of maximum possible density is understandable, since APDS sub-projectiles operate by the principle of KEP (*Kinetic Energy Penetrators*) [35, 36]. The drive towards improved strength properties with the maximum possible density of sub-projectile materials (where the density depends on the tungsten content in the alloy) has a negative impact on the properties determined under dynamic loads.

Hence the continued attempts at developing a technology which would ensure that WHAs retain high strength parameters, an optimum resistance to dynamic loads, and the maximum possible density.

2. MATERIALS AND RESEARCH METHODOLOGY

The research into the effect of chemical composition and manufacturing process was carried out on two WHAs with the chemical composition W91-Ni6-Co3 and W91-Ni6-Co2.25-Fe0.75 (% m/m), respectively, and respectively designated PR200 and PR201. WHA PR200 had the nickel to cobalt ratio of 2:1, whereas WHA PR201 had a part of the cobalt content replaced with iron. The mass fraction of tungsten in both WHAs was 91% (m/m), which ensured the required density of the material at 17.4 g/cm^3 . The mass ratios of the alloy elements and a proper selection of heat treatment and plastic forming operations should produce a microstructure which follows: tensile strength, $R_m > 1400 \text{ MPa}$, proof stress, $R_{p0.2} > 1350 \text{ MPa}$, elongation, A_5 at minimum 11%, impact strength, $KC > 115 \text{ J/cm}^2$, and hardness $> 40\text{HRC}$. The test materials in the form of rods were fabricated at the Laboratory of Heavy Alloys of the Department of Mechanical Engineering and Armament Technologies at the Warsaw University of Technology, Faculty of Production Engineering (Poland).

The first stage of WHA manufacturing was batching powdered W, Ni, Fe, and Co at an accuracy of 1 gram. Next, the powders were mixed for 20 hours in a drum mixer to achieve proper uniformity. The mixing time was specified from prior testing of the mixing times from 2 h to 24 h. The next stage was steel die pressing in 6 kg batches of the mixture. The die pressing machine was a Voehler angle press applying 200 MPa. This provided P/M compacts in the form of rods approximately 38 mm in diameter and 550 mm in length. The P/M compacts were laid on a bed of powdered Al_2O_3 deposited on a molybdenum tray and moved to a Vacuum Industries chamber furnace for hydrogen gas sintering in a predefined processing cycle. The hydrogen gas sintering was an LPS process which took 20 minutes at 1530°C .

Following the LPS process, the rods were heat treated to endow the WHA with plasticity sufficient for cold forming. The heat treatment was processed in a vacuum chamber at 5 Pa and between the temperatures of 950 and 1150°C . Following this annealing process, which took a total of 9 hours, the rods were removed, and flash cooled in water. The annealing time and temperature were specified from prior proprietary experiments, pilot tests, analysis of W-Ni-Co ternary balance, and reference data [1-3, 18-25].

The next manufacturing stage had the WHA rods cold formed on a four-lever swager with a draft of 19-35%.

The resulting WHA rods were tested for geometrical features, post-LPS density, mechanical properties and the appearance of the microstructure. The mean density of each WHA grade was determined from a series of three tests on each WHA rod. The density tests provided critical information to validate the LPS process. If the post-LPS WHA had a density lower than the theoretical value, it would mean that discontinuities were present in the rods. The density was tested and measured on a hydraulic balance. The mechanical properties were determined in static tensile tests on an Instron 1115 machine. The objective of the tests was to determine the values of tensile strength, R_m , proof stress, $R_{p0.2}$, and elongation, A_5 . The tests were performed on quintuple round specimens with a gauge diameter of 6 mm and excised on the WHA rod axis. Impact resistance was tested with a Charpy drop hammer machine, equipped with a ram at initial energy of 300 J. These tests were performed on non-notched specimens with a cross section of 10x10 mm. Hardness was tested with a Rockwell universal hardness testing machine and in scale C. The hardness tests were performed in a plane perpendicular to the WHA rod axis and on 8-10 mm thick specimens excised on the WHA rod axis. The specimens were prepared for the hardness testing by grinding the surfaces of interest to ensure proper flat parallelism and finish.

The microstructure was examined by metallographic inspection and under a SEM (scanning electron microscope). The metallographic inspection was carried out on polished sections perpendicular and parallel to the WHA rod axis in the as-LPS processed condition, after heat treatment and after heat treatment with plastic forming. The metallographic inspection was done under an Olympus IX-70 metallographic inspection microscope and a Nikon Eclipse MA200 microscope. Selected specimens made from WHA rods passed SEM fractography. The examination was done on the specimen fractures produced by breaking during the tensile tests or the impact strength tests. The objective of the examination was to understand the nature of fracture and whether the failure was brittle, plastic, or brittle and plastic. The fractographic examination and imaging were done with LEO 1530 SEM at 500x, 1000x and 5000x magnification.

3. TEST RESULTS

3.1. Test results of mechanical properties

Figure 1 features the photographs of the WHA rods after the LPS process. The photographs show that the WHA rods featured a shiny surface (Fig. 1a) and no cross-sectional geometry changes were evident (Fig. 1b). The geometric tests revealed that the length and diameter of the post-LPS WHA rods were approximately 450 mm and 31 mm, respectively.

The length measurements of the pre-LPS and post-LPS WHA rods confirmed that the linear shrinkage in the post-LPS condition was 18%.

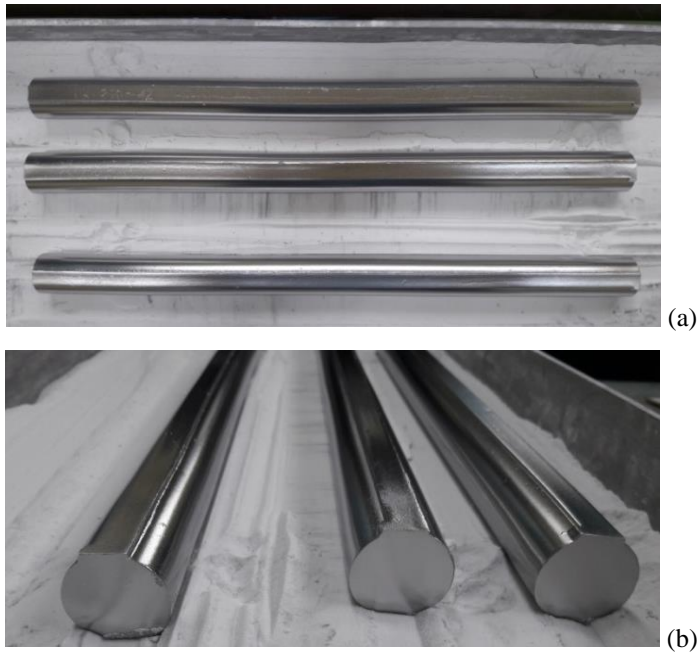


Fig. 1. Overview of the WHA rods after the LPS process. The WHA rods are placed on an Al_2O_3 powder bed in a molybdenum tray

The actual density test results for the post-LPS condition are shown in Table 1. Table 1 reveals that the actual density was virtually the same as the design (theoretical) density. The hardness of both post-LPS WHA grades revealed slight variations.

Table 1. Post-LPS density and hardness test results

WHA	Designation	Design density [g/cm ³]	Actual density [g/cm ³]	Hardness [HRC]
W91Ni6Co3	PR200	17.46	17.50 ± 0.01	32 ± 0.9
W91Ni6Co2.25Fe0.75	PR201	17.43	17.44 ± 0.01	31 ± 1.2

Table 2 lists the test results of the PR200 and PR201 WHAs after the heat treatment. Table 2 clearly shows that the ternary 91WNi6Co3 alloy grade (where both grades were heat treated identically) had a much better combination of strength (R_m and $R_{p0.2}$) and plastic formability (A_5) than the 91WNi6Co2.25Fe0.75 alloy grade.

What was also important is that the PR200 WHA had a better impact strength than the PR201 WHA. Figure 2 shows a PR200 specimen after the hardness test.

Table 2. Test results for the post heat treatment WHA mechanical properties

WHA	Hardness [HRC]	Tensile strength, R_m [MPa]	Proof stress, $R_{p0.2}$ [MPa]	Unit elongation, A_5 [%]	Impact strength, KC [J/cm^2]
PR200 (no. of specimens)	34 ± 0.8 (5)	1160 ± 5.6 (5)	820 ± 4.3 (5)	33 ± 0.9 (5)	> 300 * (6)
PR201 (no. of specimens)	33 ± 0.7 (5)	1080 ± 7.3 (5)	780 ± 4.8 (5)	27 ± 1.1 (5)	270 ± 19.2 (6)

* – out of the six impact strength specimens, four did not break (Fig. 2); the impact strength values of the broken specimens were: 285 and 290 J/cm^2 .



Fig. 2. Overview of an unbroken specimen following a hardness test with a ram at the initial energy of 300 J.

Table 3 lists the test results of the mechanical properties of the PR200 and PR201 WHAs after the plastic forming process. The test results are shown for two drafts: 19% and 24% in PR200, and 19% and 35% for PR201. A comparison of the PR200 test results at 24% of draft to the PR201 test results at 35% of draft was chosen because these draft values made the tensile test results comparable.

Table 3 shows that cold forging applied in the plastic forming process greatly improved the strength properties, and — as expected — the improvement was direct with the draft size. The increase of strength reduced the plastic formability properties.

Table 3. Mechanical properties of the PR200 and PR201 WHAs following the forging process

WHA	Draft [%]	Hardness [HRC]	Tensile strength, R_m [MPa]	Proof stress, $R_{p0.2}$ [MPa]	Unit elongation [%]	Impact strength, KC [J/cm ²]
PR200 (no. of specimens)	19	45 ± 0.9 (4)	1420 ± 8.8 (6)	1390 ± 5.8 (6)	12.8 ± 1.2 (6)	158 ± 54 (7)
	24	46 ± 0.8 (5)	1470 ± 10.2 (7)	1400 ± 9.3 (7)	10.8 ± 1.8 (7)	138 ± 60 (8)
PR201 (no. of specimens)	19	43 ± 0.8 (5)	1220 ± 11.6 (6)	1200 ± 10.3 (6)	11.9 ± 1.3 (6)	90 ± 14 (7)
	35	43 ± 0.9 (5)	1370 ± 13.2 (6)	1360 ± 13.8 (6)	6.6 ± 1.5 (6)	62 ± 15 (6)

A noticeably better combination of strength and plastic forming properties was produced in the ternary alloy, unlike in the Fe alloy grade. This difference is significant; more importantly, the PR200 WHA met the test assumptions, whereas the PR201 WHA failed to achieve the specified mechanical resistance or impact strength, even at high draft values.

3.2. Metallographic examination results

The figures below show the metallographic images of the lengthwise polished sections on the WHA rod axis. The images show the microstructure of the 91WNi6Co3 (PR200) WHA and the 91WNi6Co2.25Fe0.75 (PR201) alloy in the post-LPS and heat treatment condition (Fig. 3) and in the post-LPS, heat treatment and plastic forming condition (Fig. 4). While the microstructure was similar in PR200 and PR201 in terms of tungsten grain shape, the matrix varied significantly between the WHAs. The difference was the presence of fine precipitates in the PR200 matrix which could not be found in the PR201 matrix (which featured iron). The fine precipitates were most likely an intermetallic phase type $(Ni,Co)_3W$ or $(Co,Ni)_7W_6$ [19, 34]. It would explain the better strength of the ternary WHA over the quaternary WHA. The fine precipitates provided dispersion hardness of the matrix that was not present in the 91WNi6Co2.25Fe0.75 WHA.

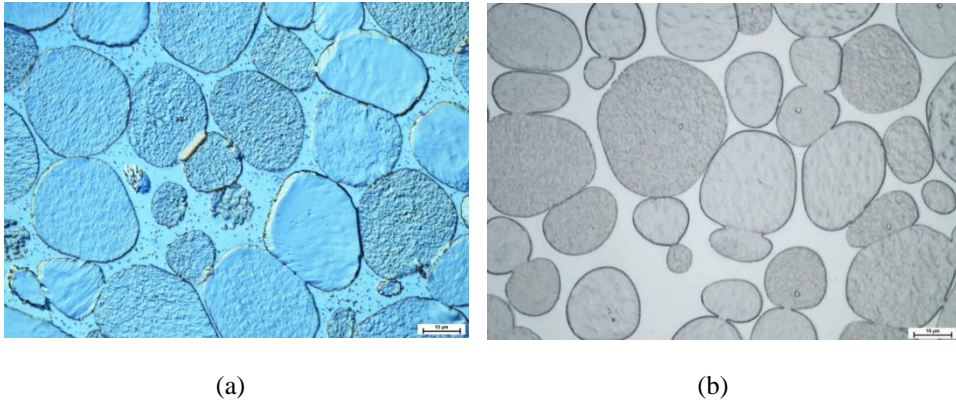


Fig. 3. Microstructure of (a) PR200 and (b) PR201 in the post heat treatment condition and developed on the polished sections in parallel to the WHA rod axis.

The microstructure in the WHA s following the plastic forming process (Fig. 4) was not distinctively different from the microstructure in the WHAs following the heat treatment (Fig. 3). The cold-forged WHA revealed a slight deformation of the tungsten grains, which took on an elliptic geometry. Nevertheless, the very fact that some tungsten grains were deformed proved that the hardening of the matrix achieved a value above the yield stress of tungsten, which most probably occurred in the grains with an optimal orientation relative to the applied external stress.

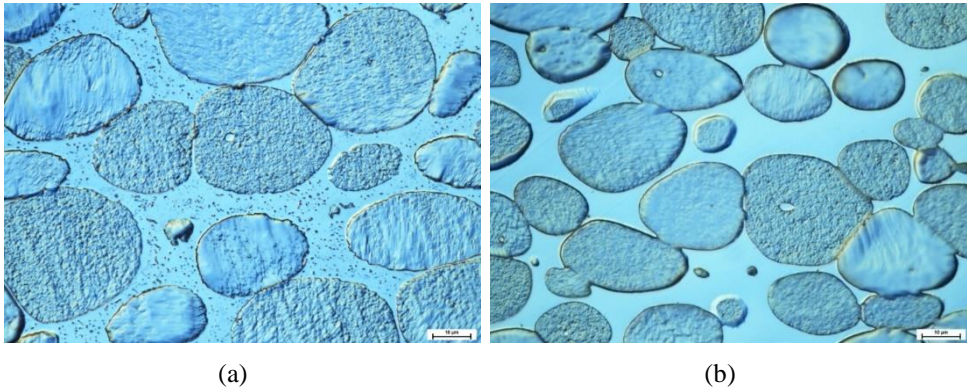


Fig. 4. Microstructure of PR200 and PR201 in the post heat treatment and plastic forming condition and developed on the polished sections in parallel to the WHA rod axis

3.3. SEM examination results

Figure 5 shows examples of the SEM imaging of the change in the nature of the PR200 fracture surface in reference to the applied processing of the specimens. The examination revealed that the fractures produced directly following the LPS process had the features of low-energy brittle fracture along the tungsten-matrix (W-m) interface and the tungsten-tungsten (W-W) grain interface.

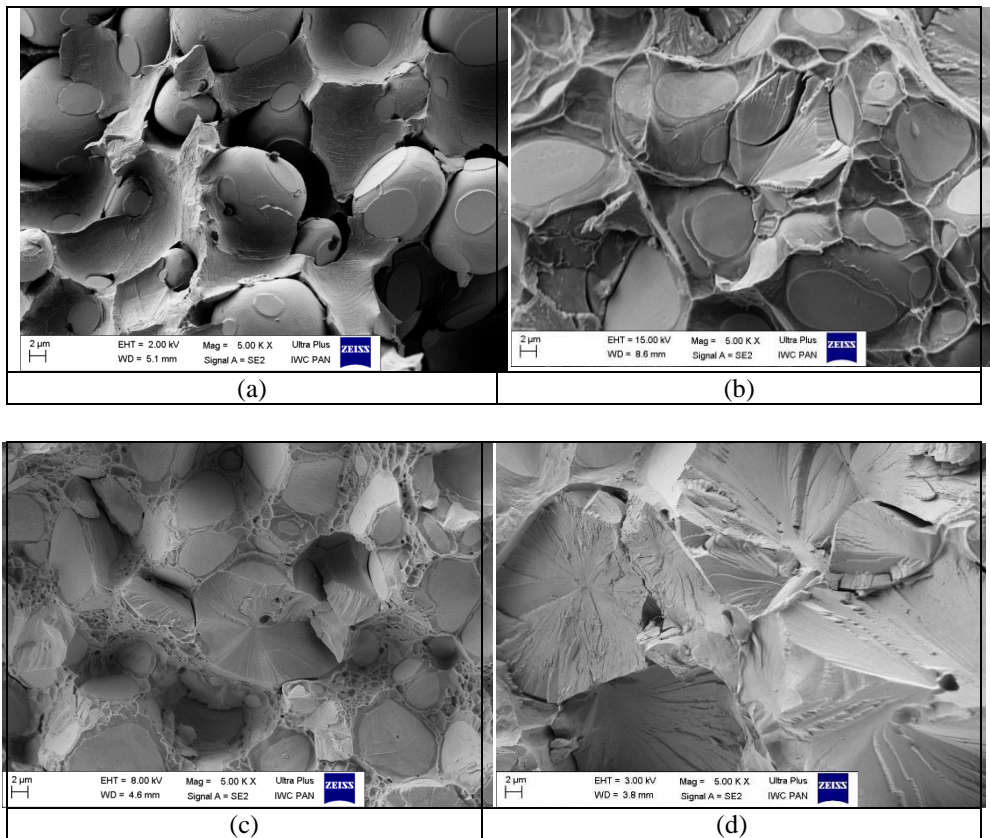


Fig. 5. SEM images of the fracture surfaces in WHAs directly following (a) the LPS process, (b) the heat treatment, and (c, d) the heat treatment and plastic forming processes

A result of the low-energy brittle fracture were smooth partition surfaces and no deformation in the binder phase (Fig. 5a). The specimen fractures in the post heat treatment condition (Fig. 5b) were dominated by fractures along the W-W grain interface and through the binder phase.

An effect of the latter fractures was a feathered matrix with plastic deformations. Isolated, singular intracrystalline fractures through the tungsten grains were also evident. The WHA specimens in the post heat treatment and plastic forming condition were dominated by intracrystalline fractures through the tungsten grains (Fig. 5d). There were fractures visible through the hardened matrix, and fractures along the low-energy W-W interface (Fig. 5c).

4. DISCUSSION OF THE TEST AND EXAMINATION RESULTS

This paper features selected test and examination results for two WHAs, 91WNi6Co3 (designation PR200) and 91WNi6Co2.25Fe0.75 (designation PR201). The calculated design density of the WHAs, without consideration of the formation of solid solution, was 17.46 g/cm^3 in PR200 and 17.43 in PR201. The actual density was 17.50 g/cm^3 in PR200 and 17.44 in PR201. The Rockwell hardness tested directly in the post-LPS condition was 34 HRC in PR200 and 33 HRC in PR201. The tests of mechanical properties of the Fe-free PR200 WHA gave a tensile strength, $R_m = 1160 \text{ MPa}$, a proof stress, $R_{p0.2} = 820 \text{ MPa}$, an elongation, $A_5 = 33\%$, and a hardness of 34 HRC. Note that the heat treatment process applied so far and consisting in annealing of the WHA rods at temperatures of $1100\text{-}1200^\circ\text{C}$ for 4 to 9 h produced a tensile strength, R_m , of 1000 MPa in both WHAs. The modified heat treatment applied could provide a tensile strength higher by approximately 160 MPa in PR200 and approximately 80 MPa in PR201.

Many the hardness test specimens of PR200 WHA with $10 \times 10 \text{ mm}$ in cross section did not break during the hardness tests. This means that the produced impact strength of the specimens of PR200 WHA was above 300 J/cm^2 .

For PR201, which featured Fe, the values of all post heat treatment parameters were lower: $R_m = 1080 \text{ MPa}$, $R_{p0.2} = 780 \text{ MPa}$, $A_5 = 27\%$, hardness of 33 HRC. The impact strength of the WHA was $KC = 270 \text{ J/cm}^2$.

The plastic forming of PR200 with a draft of 19% provided $R_m = 1420 \text{ MPa}$, $R_{p0.2} = 1390 \text{ MPa}$, and $A_5 = 12.8\%$. The increase of draft to 24% gave an increase in R_m of 50 MPa, a slight increase of proof stress (10 MPa), and reduced the elongation below the specified minimum, down to $A_5 = 10.8\%$. For PR200, the impact strength was $158 \pm 54 \text{ J/cm}^2$ (at 19% of draft) and $138 \pm 60 \text{ J/cm}^2$ (at 24% of draft).

The tensile strength in PR201 forged with a draft of 19% was 200 MPa lower than in PR200. The increase of draft to 35% gave an increase in R_m to 1370 MPa with an elongation of 6.6% and an impact strength of $62 \pm 15 \text{ J/cm}^2$.

The impact strength results presented for the PR200 WHA had a large scatter of values, which most likely was partial to the potential for microfracture development within the material during the forging process.

5. CONCLUSION

The tests and examinations discussed here allow the following conclusions:

1. The applied LPS parameters enabled the production of non-porous materials with developed elliptic tungsten grains which were uniformly distributed in the matrix.
2. The modified heat treatment process helped improve the W91Ni6Co3 WHA strength properties by approximately 150 MPa above the values possible in traditional heat treatment.
3. The selection of an optimized chemical composition, coupled with the heat treatment and the plastic forming at 20% of draft, produced an WHA with a density above 17.4 g/cm³ which met the specified mechanical criteria.
4. The W-Ni-Co ternary alloy developed better hardening by plastic forming than the W-Ni-Co-Fe quaternary alloy at the same draft.
5. The most effective draft for the W-Ni-Co ternary alloy, which provided the highest increase of strength parameters was approximately 20%. Any further increase in draft reduced the increment of tensile strength and caused the plasticity below the minimum criterion.

FUNDING

This paper features the results of research funded by the Polish National Centre for Research and Development under the project titled "Opracowanie i wykonanie demonstratorów technologii krytycznych elementów do nowej generacji amunicji czołgowej 120 mm" (Development and implementation of critical technology demonstrators for the new generation of 120 mm tank artillery ammunition) and carried out for national defence and security under Competition No. 8/2016. Contract no. DOB-BI08/05/01/2016.

REFERENCES

- [1] Kumari Anjali, M. Sankaranarayana, T.K. Nandy. 2017. "On structure property correlation in high strength tungsten heavy alloys". *International Journal of Refractory Metals & Hard Materials* 67 : 18-31.
- [2] Ravi U. Kiran, A. Panchal, M. Prem Kumar, M. Sankaranarayana, G.V.S. Nageswara Rao, T.K. Nandy. 2017. "Refractory metal alloying: A new method for improving mechanical properties of tungsten heavy alloys". *Journal of Alloys and Compounds* 709 : 609-619.
- [3] Chun-Liang Chen, Shih-Hsun Ma. 2017. "Effects of Ni/Co ratio and mechanical alloying on characteristics and sintering behavior of W-Ni-Co tungsten heavy alloys". *Journal of Alloys and Compounds* 711 : 488-494.

- [4] Kumari Anjali, G. Prabhu, M. Sankaranarayana, T.K. Nandy. 2017. "Effect of solution treatment temperature and cooling rate on the mechanical properties of tungsten heavy Allom". *Materials Science & Engineering A* 688 : 225–236.
- [5] Bagchi T.P., P. Ghosal, K. Muraleedharan, B. Sarma, N. Maitra. 2010. "Development of W-Ni-Co heavy alloy system". *P/M Science & Technology Briefs*, 2 (4) : 21-24.
- [6] Gong X., J.L. Fan, F. Ding, M. Song, B.Y. Huang. 2012. "Effect of tungsten content on microstructure and quasi-static tensile fracture characteristics of rapidly hot-extruded W-Ni-Fe alloys". *International Journal of Refractory Metals and Hard Materials* 30 (1) : 71-77.
- [7] Ravi Kiran U., A. Sambasiva Rao. 2012. "Swaging and heat treatment studies on sintered 90W-6Ni-2Fe-2Co tungsten heavy alloy". *International Journal of Refractory Metals and Hard Materials* 33 : 113-121.
- [8] Ravi Kiran U., S. Venkat, B. Rishikesh. 2013. "Effect of tungsten content on microstructure and mechanical properties of swaged tungsten heavy alloys". *Materials Science & Engineering A* 582 : 389-396.
- [9] Katavić Boris, Zoran Odanović. 2008. "Investigation of the rotary swaging and heat treatment on the behavior of W- and γ - phase in PM 92,5W-%-Ni-2,5Fe-0,26Co heavy alloy". *Materials Science and Engineering A* 492 : 337-345.
- [10] Katavić Boris, Milutin Nikačević, Zoran Odanović. 2008. "Effect of cold swaging and heat treatment on properties of the P/M 91W-6Ni-3Co heavy alloy". *Science of Sintering* 40 : 319-331.
- [11] Das Jiten, G. Appa Raoa, S.K. Pabi. 2011. "Deformation behaviour of a newer tungsten heavy alloy". *Materials Science and Engineering A* 528 : 6235-6247.
- [12] German M. Randall. 1985. *Liquid phase sintering*. New York: Plenum Press.
- [13] Ludyński Zbigniew, Waldemar Nowak. 1995. "Spieki ciężkie - technologia i właściwości". *Metalurgia Proszków XXVIII* (3/4) : 24-28.
- [14] Kaczorowski Mieczysław, Zbigniew Ludyński, Paweł Skoczylas, Waldemar Nowak, Mirosław Rafalski. 2007. "Badania właściwości kompozytów wolframowych wykonanych z różnie przygotowanych mieszanek. Część I. Badania właściwości fizycznych mieszanek proszków". *Rudy i metale nieżelazne* 52 (9) : 560-565.
- [15] Włodarczyk Edward, Adam Jackowski, Jerzy Michałowski, Jan Piętaszewski, Stanisław Malinowski. 2000. "Zależność właściwości spieków ciężkich z osnową wolframową od parametrów prasowania i rodzaju mieszanek proszkowych". *Biuletyn WAT* 49 (12) : 81-105.

- [16] Humail I.S., F. Akhtar, S.J. Askari, M. Tufail. 2007. "Tensile behavior change depending on the varying tungsten content of W-Ni-Fe alloys". *International Journal of Refractory Metals & Hard Materials* 25 : 380 - 385.
- [17] German M. Randall. 2010. Thermodynamics of sintering. In *Sintering of Advanced Materials* (Ed. Zhigang Zak Fang) 3-32. Woodhead Publishing.
- [18] Kaczorowski Mieczysław, Paweł Skoczylas, Waldemar Nowak, Mirosław Rafalski. 2008. "The study of hardening weight heavy alloys". *Archives of Foundry Engineering* 8 (1) : 167-174.
- [19] US Patent 5462576: *Heavy metal alloy and method for its production* (1995).
- [20] Hyung B.W., H.M. Hee, K.E Pyo. 2006. "Heat treatment behavior of tungsten heavy alloy". *Solid State Phenomena*, 118 : 35-40.
- [21] Katavić Boris, Milutin Nikačević, Zoran Odanović. 2008. "Effect of cold swaging and heat treatment on properties of the P/M 91W-6Ni-3Co heavy alloy". *Science of Sintering* 40 : 319-331.
- [22] Kaczorowski Mieczysław, Waldemar Nowak, Paweł Skoczylas, Mirosław Rafalski. 2016. Badania nad wytwarzaniem rdzeni podkalibrowych pocisków przeciwpancernych kaliber 120mm. W *Materiały XV Konferencji Naukowo – Technicznej Problemy Rozwoju, Produkcji i Eksploatacji Techniki Uzbrojenia* 219-232. Rynia, maj 2006.
- [23] US Patent 529426. *Repeated sintering of tungsten based heavy alloys for improved impact toughness* (1994).
- [24] Moon Hee Hong, Scong Lee, Joo-Woong Noh. 1994. The effect of thermo-mechanical treatment on the microstructure and failure behavior of sintered W heavy alloy. In *Advances in powder metallurgy and particulate materials* 5 : 279÷288.
- [25] Kaczorowski Mieczysław, Paweł Skoczylas, Mirosław Rafalski i in. 2007. *Badania amunicji o niekonwencjonalnych zastosowaniach-Badania wpływu obróbki cieplno-mechanicznej na strukturę i własności mechaniczne kompozytów wolframowych*. Politechnika Warszawska.
- [26] Don-Kuk Kim, Sunghak Lee, Joon-Woong Noh. 1998. "Dynamic and quasi-static torsional behavior of tungsten heavy alloy specimens fabricated through sintering, heat-treatment, swaging and aging". *Materials Science and Engineering* A247 : 285–294.
- [27] http://imik.wip.pw.edu.pl/zmitu/index.php?option=com_content&task=blogcategory&id=47&Itemid=36/ (2018).
- [28] <http://www.moly-china.com/products/Tungsten-Heavy-Alloy.html/> (2018).
- [29] <http://en.chinatungstenball.com/product.asp?ClassID=9/> (2018).
- [30] https://www.wolfmet.com/wp-content/uploads/2017/01/Wolfmet-Aerospace-brochure-NEW-version8_HR.pdf/ (2018).

- [31] <https://www.plansee.com/en/materials/tungsten-heavy-metal.html/> (2018).
- [32] <https://www.kennametal.com/en/home.html/> (2018).
- [33] <http://www.atm-tungsten.com/english/product.php?tid=320/> (2018).
- [34] Skoczylas Paweł. 2013. *Wpływ dodatku kobaltu na strukturę i właściwości mechaniczne wolframowych stopów ciężkich*, Rozprawa doktorska. Warszawa: Politechnika Warszawska.
- [35] Yadav S., K.T. Ramesh. 1997. The dynamic behavior of a tungsten-hafnium composite for kinetic energy penetrator applications. In *Proceedings of the 4th International Conference on Tungsten Refractory Metals and Alloys* 111-117.
- [36] Magness L.S., D. Kapoor. 1994. "Flow-softening tungsten composites for kinetic energy penetrator applications". *Tungsten and Refractory Metals* 11-20.

Badania procesu wytwarzania wolframowych stopów ciężkich o wymaganych właściwościach mechanicznych

Paweł SKOCZYLAS, Zbigniew GULBINOWICZ, Olgierd GOROCH,
Katarzyna BARCZ, Mieczysław KACZOROWSKI

*Politechnika Warszawska, Wydział Inżynierii Produkcji
ul. Narbutta 85, 02-524 Warszawa*

Streszczenie. Przedmiotem niniejszego pracy, zrealizowanej w ramach projektu NCBiR i zatytułowanego "Opracowanie i wykonanie demonstratorów technologii krytycznych elementów do nowej generacji amunicji czołgowej 120mm" są wyniki badań wpływu parametrów spiekania z udziałem fazy ciekłej - LPS (ang. *Liquid Phase Sintering*) oraz obróbki cieplnej na właściwości mechaniczne stopów W91Ni6Co3 oraz W91Ni6Co2,25Fe0,75 oznaczonych odpowiednio symbolami PR200 oraz PR201. Wytypowane stopy, po spiekanii oraz obróbce cieplnej, były badane na maszynie wytrzymałościowej celem wyznaczenia wytrzymałości na rozciąganie (R_m), umownej granicy plastyczności ($R_{p0,2}$) oraz wydłużenia (A_5). Na podstawie analizy wyników badań zaproponowano parametry procesu wytwarzania umożliwiające uzyskanie przez badane stopy wymaganych właściwości mechanicznych. Stwierdzono, iż z punktu widzenia tych właściwości, bardziej perspektywiczny jest trójskładnikowy stop o składzie chemicznym W91Ni6Co3 oznaczony symbolem PR200. Stop ten, po spiekanii i dwustopniowej obróbce cieplnej umożliwia uzyskanie materiału o wytrzymałości na rozciąganie $R_m > 1400$ MPa, umownej granicy plastyczności $R_{p0,2}$ powyżej 1350 MPa, wydłużeniu minimum 11% oraz udarności $KC > 115$ J/cm².

Słowa kluczowe: wolframowe stopy ciężkie (WSC), spiekanie z udziałem fazy ciekłej, właściwości mechaniczne, kinetyczne penetratory energii, wysokowytrzymałe WSC